Photonic angle-of-arrival and time-difference-of-arrival measurement based on dual drive 1×2 MZM

Yi Ni (倪 屹)[1*], Xuan Kong (孔 轩)[1], Ruixin Wang (王瑞鑫)[2], Yitang Dai (戴一堂)[2], and Kun Xu (徐 坤)[2]

[1] *School of IoT Engineering, Jiangnan University, Wuxi 214132, China*

[2] *School of Information and Communication Engineering, Beijing 100876, China*

[*] *Corresponding author: niy2011@163.com*

Received November 15, 2012; accepted December 20, 2012; posted online February 28, 2013

We propose and experimentally demonstrate a photonic approach to estimate the time-difference-of-arrival (TDOA) and the angle-of-arrival (AOA) of a microwave signal. TDOA and AOA are estimated from the carrier power difference of the two outputs of the Mach-Zehnder modulator (MZM) using only one dual-drive 1×2 MZM. Experimentally, the TDOA of a microwave signal at 3 GHz from 27.78 to 166.67 ps is measured with maximum measurement errors of ±2.24 ps; correspondingly, the AOA from 60° to 85.2° is measured with maximum measurement errors of ±0.4°.

OCIS codes: 060.5625, 230.0250, 300.6370.

doi: 10.3788/COL201311.030605.

Microwave receivers for radar and other electronic warfare applications require the capability to estimate the instantaneous frequency, pulse width, angle-of-arrival (AOA), and modulation format of an unknown microwave signal over a wide bandwidth. Conventional techniques used to measure these parameters are bulky, limited in bandwidth, and suffer from electromagnetic interference. Photonics offer many advantages in processing microwave signals because it has an intrinsic feature of wide instantaneous bandwidth, which is suitable for the generation, transmission, control, and processing of wideband microwave signals[1−4]. Recent studies have proposed a number of approaches for frequency estimation measurement[5−10], spectral analysis[11], and up/down-conversion of wideband microwave signals[12].

However, to date, only a few approaches have measured the critical parameters, such as the AOA and the time-difference-of-arrival (TDOA)[13,14]. In Ref. [13], the phase shift estimation relied on a Mach–Zehnder interferometer combined with spatial-spectral (S2) materials. Through the spectral analysis function of the S2 materials, the high resolution optical spectrum is obtained, through which different powers are detected in the sidebands related to the phase of the radio frequency (RF) signals and the time delay information. In Ref. [14], the microwave signals are received by a cascade of two Mach–Zehnder modulators (MZMs), and TDOA and AOA are equivalently converted into a phase shift between two replicas of the received signals at two modulators. Through proper biasing of the two MZMs, the total optical power of the carrier wavelength at the output is obtained as a function of phase shift. However, the perturbations of fiber length between the two MZMs are influenced by the environment.

In this letter, a novel photonic AOA and TDOA measurement scheme is proposed. In our scheme, TDOA and AOA are calculated from the phase shift of the two copies of a microwave signal which are modulated onto the two arms of the dual-drive 1×2 MZM. The phase shift is a function of the average carrier power difference of the two outputs of MZM, which is received by a balanced photo detector (BPD), and calculated from the direct current (DC) component of the photo current. The phase shift is estimated through the optical power in Ref. [14], so these two schemes are essentially different. The key significance of the proposed scheme is the use of only one MZM, which makes the system compact, stable, and inexpensive. Moreover, signal processing (DC component extraction) can be simply implemented by an integrator, which is favorable for real-time operation.

The proposed approach is schematically shown in Fig. 1. The system consists of a continuous wave (CW) laser, a dual-drive 1×2 MZM, a BPD, a filter, and an integrator. The microwave signals with phase difference (i.e., φ) are received by antennas, amplified to a predefined power level, and then modulated onto the two arms of the MZM. In the MZM, the CW laser is first split into two parallel paths and phase modulated by the two copies of the received signal whose phase difference is dependent on AOA. The two light paths are then recombined to interfere with each other at the output of the 1×2 MZM, which is equivalent to a 2×2 coupler. The power difference at the carrier wavelength is a function of the phase shift because of the phase difference between the two phase-modulated components. Thus, the phase shift can be estimated, and TDOA and AOA can be measured by equally detecting the power at the carrier wavelength,

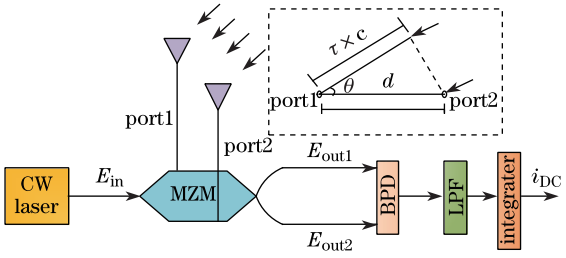

Fig. 1. Schematic of the proposed approach. Inset: illustration of TDOA and AOA. LPF: low-pass filter.

such as the DC component of the BPD's photo current. MZM is biased to ensure that one optical path is at the minimum transmission point, whereas the other output is complemented to maximize the carrier power difference at BPD.

The signals received by an antenna array experience a RF delay, which depends on the angle of the RF wavefront. The relationship between AOA and TDOA follows that described in Ref. [14], which is shown in the inset of Fig. 1. Assuming that AOA is θ, TDOA is given by $\tau = d\cos\theta/c$, where d is the distance between the two receiving antennas and c is the light velocity in vacuum. An equation related to TDOA, AOA, and the frequency-dependent phase shift φ, is given by

$$\omega\tau = \varphi + 2k\pi, \theta = \cos^{-1}(\tau c/d), \tag{1}$$

where ω is the angular frequency of the microwave signal. Assuming an ideal 50/50 input and output couplers of the 1×2 MZM, the output optical signals with electric fields E_{out1} and E_{out2} related to the input optical electric field E_{in}[15], and the received microwave signals are given by

$$\begin{bmatrix} E_{\text{out1}} \\ E_{\text{out2}} \end{bmatrix} \propto \begin{bmatrix} 1 & \text{i} \\ \text{i} & 1 \end{bmatrix} \cdot \begin{bmatrix} \text{e}^{\text{j}\left[\beta_1 \sin(\omega t)+\varphi_{\text{dc}}\right]} & 0 \\ 0 & \text{e}^{\text{j}\beta_2 \sin(\omega t+\phi)} \end{bmatrix} \begin{bmatrix} 1 & \text{i} \\ \text{i} & 1 \end{bmatrix} \begin{bmatrix} E_{\text{in}} \\ 0 \end{bmatrix}, \tag{2}$$

where $\beta_1\sin(\omega t)$ and $\beta_2\sin(\omega t)$ are the signals modulated onto the two arms, β_1 and β_2 are the modulation depths, φ is the phase difference between the microwave signal at each port, and ϕ_{dc} is the phase shift induced by the bias. The output field can be further expressed as

$$\begin{cases} E_{\text{out1}} = E_{\text{in}}\{\exp\{\text{j}[\beta_1 \sin(\omega t) + \phi_{\text{dc}}]\} \\ \qquad\qquad - \exp[\text{j}\beta_2 \sin(\omega t + \varphi)]\} \\ E_{\text{out2}} = E_{\text{in}}\{\exp\{\text{j}[\beta_1 \sin(\omega t) + \phi_{\text{dc}}]\} \\ \qquad\qquad - \exp[\text{j}\beta_2 \sin(\omega t + \varphi)]\} \end{cases}. \tag{3}$$

Through the detection of these signals with a BPD, the component of the output current is found to be proportional to

$$\begin{aligned} i_{\text{out}} &\propto \cos\left[\beta_1 \sin(\omega t) - \beta_2 \sin(\omega t + \varphi) + \phi_{dc}\right] \\ &= \cos\left[(\beta_1 - \beta_2 \cos\varphi)\sin\omega t - \beta_2 \sin\varphi \cos\omega t + \phi_{\text{dc}}\right]. \end{aligned} \tag{4}$$

After the narrow band filter and the integrator, only the DC component of the photo current is outputted; the other frequency elements in Eq. (4) are averaged out to zero in the integrator, where $A=\beta_1-\beta_2\cos\varphi$ and $B = -\beta_2\sin\varphi$. The DC component is as

$$i_{\text{DC}} \propto \cos(\phi_{\text{dc}})\left(J_0(A)J_0(B)+2\sum_{n=1}^{\infty} J_{2n}(A)J_{2n}(B)(-1)^n\right), \tag{5}$$

where J_m is the mth-order Bessel function of the first kind. According to the addition theorem of Bessel functions, the integrator DC output is given by

$$\begin{aligned} i_{\text{DC}} &\propto J_0\left(\sqrt{A^2 + B^2}\right)\cos(\phi_{\text{dc}}) \\ &= J_0\left(\sqrt{\beta_1^2 + \beta_2^2 - 2\beta_1\beta_2\cos\varphi}\right)\cos(\phi_{\text{dc}}). \end{aligned} \tag{6}$$

The two signals are amplified to predefined power levels before feeding into the MZM, so β_1 and β_2 are known. The output current of the integrator is a function of the phase shift, so the phase shift can be estimated by measuring the DC component of the output from BPD. In addition, TDOA and AOA can be calculated based on Eq. (1). The bias point of MZM also affects the measuring result in Eq. (6), so we choose the bias point where one optical path is at the minimum transmission and the other is at the maximum, in which case the output DC is maximized and the control of bias can be carried out by simply monitoring the maximal or minimal optical power at the outputs in the absence of RF modulation. The calculation of phase shift is a little complex and a bias control is needed. We use the bias-control circuit to stabilize the bias point of modulation to effectively compensate for the mechanical and temperature fluctuations. Thus, the DC bias of MZM is stabilized.

To verify the proposed approach, an experiment is performed. As shown in Fig. 2, the laser source is set at 1 550 nm with an output power of 5 mW. Given the weak polarization isolation, a polarization beam splitter (PBS) is used before the modulator to ensure that the dual-drive MZM (EOspace) works at the principle state of polarization. The RF signal is generated by a RF signal generator (Anritsu MG3694B). The signal is then equally divided into two channels: the first channel directly enters through one port of MZM and the second is inputted into a phase shifter, which changes the phase difference between the two channels. Finally, the RF signal is applied to drive the MZM. In the receiving unit, the balanced detector is utilized to obtain the difference of the carrier powers. Integration is applied to the digitized data, so an oscilloscope (OSC) is used as an integrator to obtain the DC component of the BPD's output. The internal low-pass filter (LPF) with a bandwidth of 20 MHz is employed to eliminate aliasing and interference from high frequencies.

In the experiment, a phase shift between two replicas of a microwave signal at 3 GHz is applied to the different microwave input ports of the MZM to emulate the change of the TDOA and the AOA. Due to the lack of microwave amplifiers, the input powers are measured by a power meter to calculate the modulation levels, instead of amplifying them to a predefined power. The phase shift is tuned at a step of 7.2° from 30° to 180° using a manually variable polarization splitter (PS), which can display the value of the phase shift. The above phase shift range is the maximum of our (PS), which can be optimize using a better PS. The output signal of BPD is averaged many times in a large sampling time by an OSC. Therefore, the DC component (integral of the data from OSC) of the BPD output that has a fixed relationship with the phase shift is digitized.

The measured DC magnitudes corresponding to different phase shifts are shown in Fig. 3. The theoretical magnitude distribution as a function of the phase

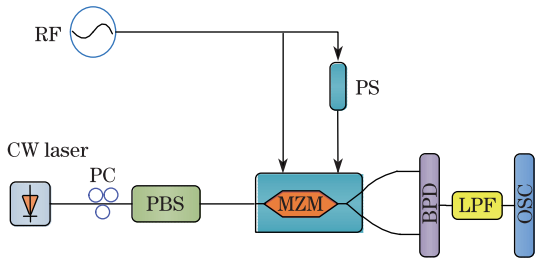

Fig. 2. Experimental setup of the proposed system. PC: polarization controller.

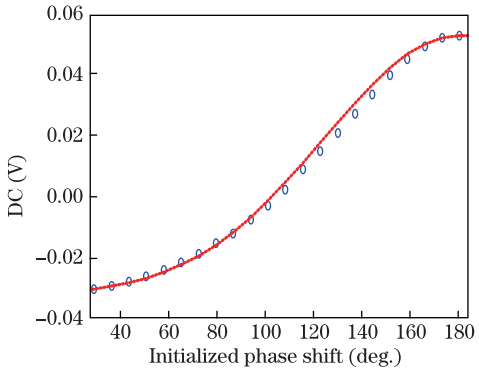

Fig. 3. Experimental results (circles) and theoretical trend for the total direct current (dashed line).

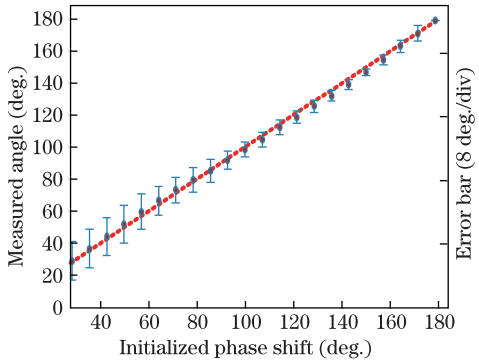

Fig. 4. Measured phase shifts (dots) and the corresponding measure errors (vertical bars) versus the initial phase shift.

shift is also shown (dashed line). The experimental data agree well with the theoretical predictions. The measured phase shifts and the measurement errors are shown in Fig. 4. The measurement errors are less than ±2.42° within the range of 30° –180°. The results are close to that in Ref. [14], which demonstrates a phase shift from –160° to 40° with measurement error less than ±2.5°. The phase error plotted in Fig. 4 is the difference between the experimental results and the theoretical results. In practical application, a PS is not needed. This phase shift is induced by the AOA of a microwave signal. After measuring the DC, the phase shift can be obtained based on Fig. 4.

TDOA and AOA can be calculated from the estimated phase shifts based on Eq. (1). We use d=0.1 m. The effective measurement range of TDOA is from 27.78 to 166.67 ps, which can be obtained from the estimated phase shifts. The measurement errors for TDOA are ±2.24 ps. AOA can be obtained from the values of TDOA, which ranges from 60° to 85.2°. The measurement errors for AOA are less than ±0.4°. A trade-off between the AOA measurement error and range can be obtained by varying the distance between the two antennas. Higher accuracy can be obtained by increasing d.

In the proposed AOA measurement system, knowledge of microwave signal frequency is critical. This information can be provided by the photonic instantaneous frequency measurement techniques to perform frequency measurement and AOA estimation[7,14].

In conclusion, a novel photonic approach to measure the TDOA and the AOA of a microwave signal is proposed and experimentally demonstrated using only one dual-drive 1×2 MZM. The proposed system has a simple structure and exhibits stable performance. The two copies of the received microwave signals are modulated onto the same MZM, so the perturbation in optical length will not affect the measurement results. Moreover, the compactness of the proposed scheme enables the reduction of size, weight, and power of the whole system. In our experiment, the phase shift from 30° to 180° is measured at 3 GHz with a maximum error of ±2.42°. The corresponding range and maximum error of AOA are 60° to 85.2° and ±0.4°, respectively.

This work was supported by the Program for New Century Excellent Talents in University (No. NCET-11-0659), the National 111 Project of China (No. B12018), and the Priority Academic Program Development of Jiangsu Higher Education Institutions.

References

1. J. Seeds and K. J. Williams, J. Lightwave Technol. **24,** 4628 (2006).
2. D. B. Hunter, M. E. Parker, and J. L. Dexter, IEEE Trans. Microw. Theory Technol. **54,** 861 (2006).
3. F. Zeng and J. P. Yao, Opt. Express **12,** 3814 (2004).
4. R. A. Minasian, IEEE Trans. Microw. Theory Technol. **54,** 832 (2006).
5. L. V. T. Nguyen and D. B. Hunter, IEEE Photon. Technol. Lett. **18,** 1188 (2006).
6. L. A. Bui, N. Sarkhosh, H. Emami, A. Mitchell, M. D. Pelusi, T. D. Vo, and B. J. Eggleton, Opt. Express **17,** 22983 (2009).
7. S. Pan and J. P. Yao, IEEE Photon. Technol. Lett. **22,** 1437 (2010).
8. X. Zou, W. Pan, B. Luo, and L. Yan, Opt. Lett. **35,** 2747 (2010).
9. Y. Dai, Y. Ji, K. Xu, Y. Li, J. Wu, and J. Lin, IEEE Photon. Technol. Lett. **24,** 661 (2012).
10. Y. Dai, K. Xu, J. Wu, Y. Li, and J. Lin, in *Proceedings of OFC 2012* OW31.3 (2012).
11. Y. Wang, H. Chi, X. Zhang, S. Zheng, and X. Jin, Opt Lett. **36,** 3897 (2011).
12. V. R. Pagán, B. M. Haas, and T. E. Murphy, Opt. Express **19,** 883 (2011).
13. Z. W. Barber, C. Harrington, C. W. Thiel, W. R. Babbitt, and R. K. Mohan, J. Lumin. **130,** 1614 (2010).
14. X. Zou, W. Li, W. Pan, B. Luo, L.Yan, and J. Yao, Opt. Lett. **37,** 755 (2012).
15. V. J. Urick, F. Bucholtz, J. D. McKinney, P. S. Devgan, A. L. Campillo, J. L. Dexter, and K. J. Williams, J. Lightwave Technol. **29,** 1182 (2011).